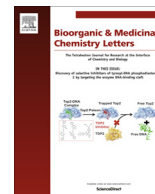




Contents lists available at ScienceDirect

## Bioorganic &amp; Medicinal Chemistry Letters

journal homepage: [www.elsevier.com/locate/bmcl](http://www.elsevier.com/locate/bmcl)

## Design, synthesis and biological evaluation of novel 5-fluoro-1*H*-benzimidazole-4-carboxamide derivatives as potent PARP-1 inhibitors

Junwei Wang<sup>a,b</sup>, Xuyan Wang<sup>b</sup>, Hui Li<sup>a</sup>, Dezhong Ji<sup>a</sup>, Yuyan Li<sup>b</sup>, Yungen Xu<sup>a,b,\*</sup>, Qihua Zhu<sup>a,b,\*</sup><sup>a</sup> Jiangsu Key Laboratory of Drug Design and Optimization, China Pharmaceutical University, Nanjing 210009, China<sup>b</sup> Department of Medicinal Chemistry, China Pharmaceutical University, Nanjing 210009, China

## ARTICLE INFO

## Article history:

Received 4 May 2016

Revised 13 June 2016

Accepted 16 June 2016

Available online xxxx

## Keywords:

PARP-1

Inhibitors

Fluorine atom

Benzimidazole

Antitumor

## ABSTRACT

A series of novel 5-fluorine-benzimidazole-4-carboxamide analogs were designed and synthesized. All target compounds were evaluated for their PARP-1 inhibitory activity. Compounds possessed high intrinsic PARP-1 inhibitory potency have been evaluated in vitro cellular assays to measure the potentiation effect of cytotoxic agents against cancer cell line. These efforts led to the identification of compound **10f**, which displayed strong inhibition against the PARP-1 enzyme with an IC<sub>50</sub> of 43.7 nM, excellent cell inhibitory activity in HCT116 cells (IC<sub>50</sub> = 7.4 μM) and potentiation of temozolomide cytotoxicity in cancer cell line A549 (PF<sub>50</sub> = 1.6).

© 2016 Published by Elsevier Ltd.

Poly ADP-ribose polymerases (PARPs), a family of 18 members, are found in nearly all eukaryotic cells.<sup>1</sup> It has been identified and characterized that PARPs participate in the process of catalyzing substrate protein ADP-ribosylation to regulate multiple processes including chromatin remodeling, transcription, DNA repair, and protein degradation.<sup>2</sup>

PARP-1 is the most abundant and well-characterized member of the family that possesses three main functional regions: DNA-binding domain, auto-modification domain, and catalytic domain. The DNA binding domain can recognize and locate the damaged DNA single-strand breaks and then bind to them to stimulate polymerization of ADP-ribose, leading to the unwinding of DNA from histones and exposing the damaged DNA for repair. The catalytic domain catalyze the transfer of ADP-ribose units from intracellular nicotinamide adenine dinucleotide (NAD<sup>+</sup>) to nuclear acceptor proteins and is responsible for the formation of ADP-ribose polymers.<sup>3</sup> PARP-1 plays a key role in the repair of single strand breaks (SSB) by the base excision repair (BER) pathway, especially in tumor cells with BRCA1/2-deficient and lack of homologous recombination (HR) repair.<sup>4</sup> It is generally accepted that the catalytic activity of PARP-1 is stimulated by DNA damage caused by ionizing radiation, chemotherapy, UV light, or products of cellular and oxidative

metabolism, thus it is regarded as a target for treating diseases related to ischemia–reperfusion injury and cancer.<sup>5</sup>

It is clear that the vast majority of PARP-1 inhibitors are based on the benzamide as pharmacophore, which mimics the nicotinamide moiety of NAD<sup>+</sup> binding mode, by conformational restriction of a primary amide or by transformation of an amide into a lactam. Nicotinamide and 3-aminobenzamide were the earliest PARP-1 inhibitors, however, their low potency and poor specificity prompted researchers to find new PARP-1 inhibitors.<sup>6</sup> In the last three decades, a variety of PARP-1 inhibitors have been disclosed, and some of them are currently in different stages of clinical trials as single agents or in combination with DNA-damaging drugs, including veliparib, rucaparib, talazoparib and niraparib (Fig. 1).<sup>7,8</sup> Olaparib, the first PARP-1 inhibitor for treatment in patients with BRCA1/2 mutated platinum-sensitive relapsed ovarian cancer was approved by FDA and EMA in 2014.<sup>9</sup> However, many inhibitors suffer from development problems such as toxicity, poor solubility, or poor pharmacokinetic profiles.<sup>10</sup> The effort of pursuing new inhibitors with good potency against PARP-1 is still needed.

Veliparib (ABT-888), a potent small molecule inhibitor of PARP-1/2, which is cytotoxic in tumor cells with deficiencies in BRCA1 or BRCA2, is currently on-going phase III clinical trials.<sup>11</sup> However, oxidative metabolism is easy to occur on the benzimidazole moiety of veliparib, which will lead to the reduce of bioavailability.<sup>12</sup> It is a common and effective strategy to introduce fluorine atom into a

\* Corresponding authors.

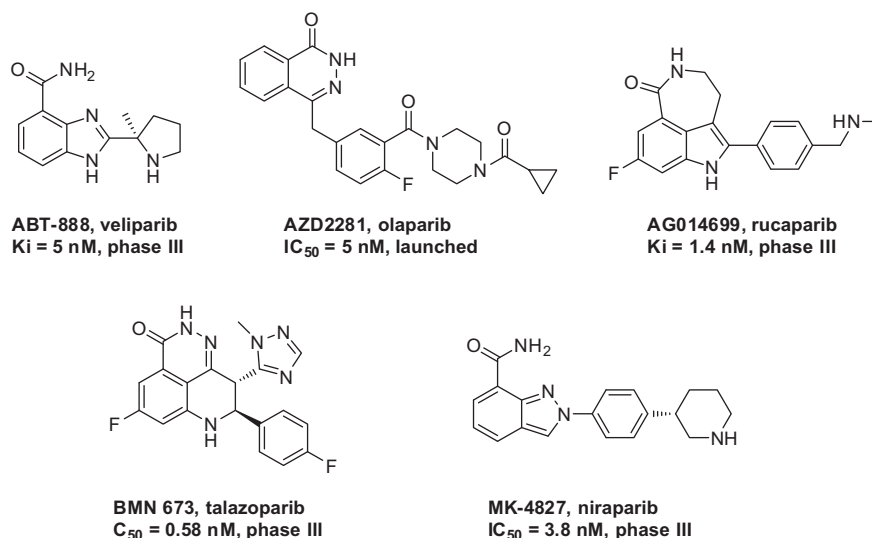


Figure 1. Structures of representative PARP-1 inhibitors.

molecule, which can productively influence conformation, pK<sub>a</sub>, intrinsic potency, membrane permeability, metabolic pathways and pharmacokinetic properties.<sup>13–15</sup> In order to increase the metabolism stability of veliparib and search novel potent PARP-1 inhibitors, fluorine atom was introduced to the 5-position of benzimidazole scaffold to modulate the pharmacokinetic profiles and physicochemical properties.

On the basis of the structure–activity relationship of PARP-1 inhibitors, we designed a series of 5-fluorine-benzimidazole-4-carboxamide analogs as novel PARP-1 inhibitors. Modeling studies of compound **8b** in the catalytic domain of human PARP-1 is shown in Figure 2. The docking model (PDB code: 2RCW) revealed that the carbonyl oxygen group of **8b** can form three hydrogen bonds with Ser243, Gly202 and His201. Meanwhile, the carboxamide hydrogen exhibited hydrogen bond interaction with the backbone carbonyl oxygen of Gly202. It is obvious that the fluorine atom which was introduced to the 5-position of benzimidazole could form an additional hydrogen bond with the hydroxyl group of Ser243. This key hydrogen-bond may strengthen the interaction of ligand molecules with amino acids residues in the PARP-1 active site. In addition, the benzimidazole ring could form  $\pi$ -stacking interactions with Tyr246 and Tyr235. The docking results indicated

that the introduction of fluorine atom was favorable for the interaction between the ligand and protein active site. This result led us to design its analogs.

In order to verify our hypothesis, a series of 5-fluorine-benzimidazole-4-carboxamide derivatives were synthesized, as shown in Schemes 1 and 2. Treatment of **1** with thionyl chloride produced the corresponding acid chloride, which reacted with aqueous ammonia gave 2,6-difluorobenzamide **2**. Nitration of **2** with mixed acid of fuming nitric acid and sulfuric acid afforded nitro compound **3**, and then reaction with aqueous ammonia at room temperature gave intermediate **4**. 2,3-diamino-6-fluorobenzamide **5**, obtained by catalytic hydrogenation of **4**, was coupling with saturated nitrogen-containing heterocyclic acid under benzotriazol-1-yl-oxytripyrrolidinophosphonium hexafluorophosphate (PyBOP) or *N,N'*-carbonyldiimidazole (CDI) conditions to form intermediates **6a–e**, which were heated in acetic acid to give 5-fluorine-benzimidazole-4-carboxamide derivatives **7a–e**. Deprotection of Cbz group under catalytic hydrogenation provided secondary amines **8a–e**.<sup>16,19</sup> *N*-alkylation of **8a–e** with aldehydes or ketones under the presence of sodium cyanoborohydride afforded tertiary amines **9a–y**.<sup>17</sup>

Compounds **10a–f** were prepared according to Scheme 2. 2,3-Diamino-6-fluorobenzamide **5** was coupled with aromatic aldehyde to form **10a–e** and intermediate **11**.<sup>18</sup> Deprotection of Boc group of **11** under acidic condition provided target compound **10f**.<sup>18,20</sup>

All target compounds were evaluated in vitro for their PARP-1 enzyme inhibition activity at the concentration of 100 nM, and compounds with PARP-1 inhibitory ratio >50% were selected to determine the IC<sub>50</sub> values. The results were summarized in Table 1. Among these compounds, compound **8a**, which contained a 2-pyrrolidinyl group at 2 position, showed low inhibitory activity. While the 2-methylpyrrolidinyl derivative **8b** exhibited good potency with an IC<sub>50</sub> value of 5.7 nM, indicated that 2-methylpyrrolidinyl was an effective substituent group for PARP-1 enzyme inhibitory activity. Piperidinyl substituted analogs **8c** showed moderate PARP-1 inhibitory activity. 3- or 4-piperidinyl analogs **8d** and **8e** exhibited potent inhibitory activity against PARP-1 enzyme with IC<sub>50</sub> value of 25.8 nM and 39.1 nM, respectively. Encouraged by this result, further modification of the nitrogen atom on the pyrrolidinyl or piperidinyl group with alkyls was conducted. Among *N*-alkyl derivatives, most compounds showed weaker activity than their parent compounds. However, the

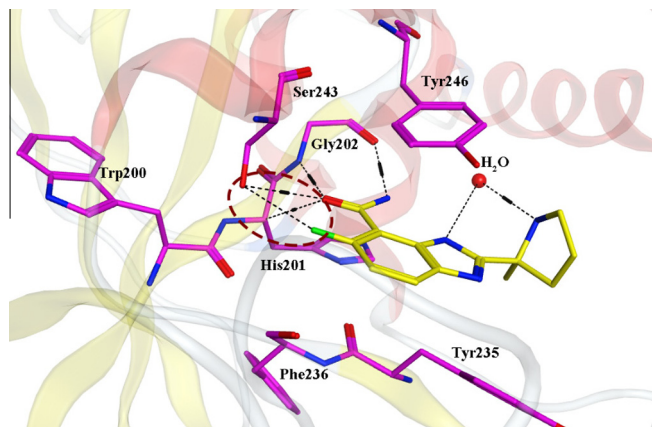
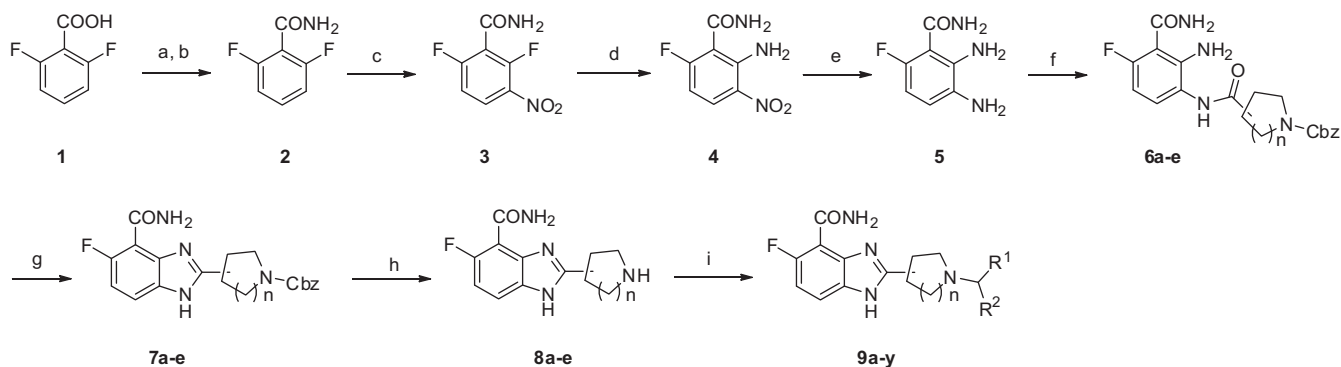
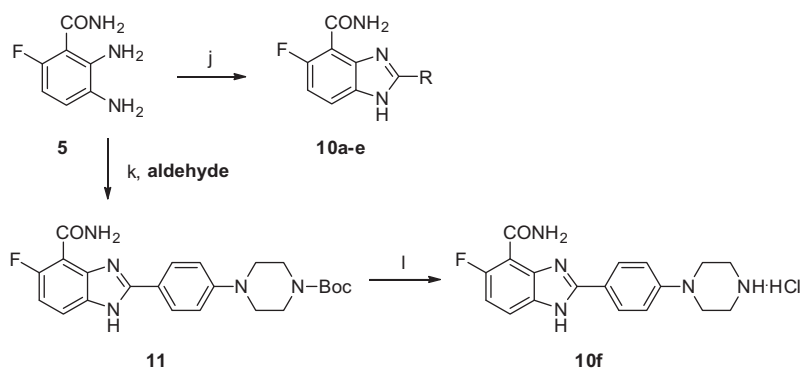


Figure 2. Docked conformation of compound **8b** into the active binding site of PARP-1. The interaction mode was obtained through molecular docking (PDB ID: 2RCW) and depicted using MOE 2013.08. The carbon atoms of the compounds and the key residues in the active site of PARP-1 were colored in yellow and purple red, respectively. The H-bonds were shown as black dot lines.



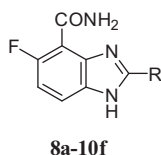
**Scheme 1.** Synthesis route for target compounds **8a–8e** and **9a–9y**. Reagents and conditions: (a)  $\text{SOCl}_2$ , reflux, 2 h; (b)  $\text{NH}_3 \cdot \text{H}_2\text{O}$ , THF, 0 °C to rt, 24 h, 90%; (c) concd  $\text{H}_2\text{SO}_4$ , fuming  $\text{HNO}_3$ , 0 °C to rt, 2 h, 92%; (d)  $\text{NH}_3 \cdot \text{H}_2\text{O}$ , EtOH, rt, 4 h, 64.1%; (e) 10% Pd–C,  $\text{H}_2$ , MeOH, rt, 12 h, 90%; (f) PyBOP, DIEA, DMF, rt, 12 h; (g) AcOH, 120 °C, 4 h, 50–72%; (h) 10% Pd–C,  $\text{HCOONH}_4$ , MeOH, rt, 2 h, 52–80%; (i)  $\text{R}_1\text{R}_2\text{C}(\text{O})$ ,  $\text{NaBH}_3\text{CN}$ , MeOH, rt, 12 h, 60–94%.



**Scheme 2.** Synthesis route for target compounds **10a–10f**. Reagents and conditions: (j)  $\text{NaHSO}_3$ ,  $\text{CH}_3\text{OH}$ , reflux, 12 h, 40–67%; (k)  $\text{NaHSO}_3$ ,  $\text{CH}_3\text{OH}$ , reflux, 12 h, 64%; (l) THF,  $\text{CH}_3\text{OH}/\text{HCl}$ , rt, 2 h, 63%.

**Table 1**

The structures and PARP-1 enzyme inhibition activity of compounds **8a–10f**



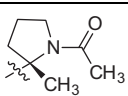
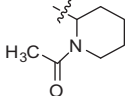
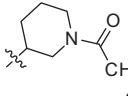
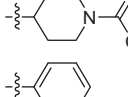
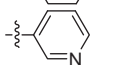
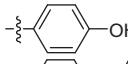
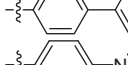
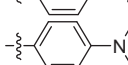


Compd	Substituents (R)	Inhibition <sup>a</sup> (%)	IC <sub>50</sub> (nM)
Veliparib		97.0	1.0
<b>8a</b>		8.5	ND <sup>b</sup>
<b>8b</b>		84.0	5.7
<b>8c</b>		44.5	ND
<b>8d</b>		59.9	25.8
<b>8e</b>		65.9	39.1
<b>9a</b>		46.6	ND

(continued on next page)

Table 1 (continued)

Compd	Substituents (R)	Inhibition <sup>a</sup> (%)	IC <sub>50</sub> (nM)
9b		15.0	ND
9c		1.9	ND
9d		4.38	ND
9e		66.1	21.7
9f		37.9	ND
9g		9.1	ND
9h		27.1	ND
9i		2.37	ND
9j		12.9	ND
9k		32.4	ND
9l		0.79	ND
9m		NA <sup>c</sup>	ND
9n		13.0	ND
9o		3.69	ND
9p		41.8	ND
9q		43.2	ND
9r		41.0	ND
9s		55.1	29.8
9t		45.3	ND
9u		NA <sup>c</sup>	ND

Table 1 (continued)

Compd	Substituents (R)	Inhibition <sup>a</sup> (%)	IC <sub>50</sub> (nM)
<b>9v</b>		4.96	ND
<b>9w</b>		6.5	ND
<b>9x</b>		4.7	ND
<b>9y</b>		2.16	ND
<b>10a</b>		27.7	ND
<b>10b</b>		3.01	ND
<b>10c</b>		21.0	ND
<b>10d</b>		6.84	ND
<b>10e</b>		66.7	21.8
<b>10f</b>		55.3	43.7

<sup>a</sup> Inhibitory ratio % at 100 nM.<sup>b</sup> ND, not determined.<sup>c</sup> NA, no activity.

*N*-methyl derivative **9a** exhibited more potent inhibition activity against PARP-1 than its parent compound **8a**. Similar to **9a**, *N*-propyl derivative **9s** (IC<sub>50</sub> = 29.8 nM) displayed similar activity with its parent compound **8e**. Compounds **9u–y**, which acyl was introduced into the nitrogen atom on the pyrrolidinyl or piperidinyl group failed to demonstrate significant inhibitory effect up to the concentration of 100 nM. In an effort to enhance potency and increase diversity of the structure, aryl substituted derivatives **10a–f** were synthesized. The phenyl substituted **10a** and pyridinyl substituted **10b** showed relatively weak PARP-1 inhibitory activity. While **10e** and **10f**, that morpholinyl and piperazinyl substituted at the *para* position of the phenyl showed good PARP-1 inhibitory activity with IC<sub>50</sub> value of 21.8 nM and 43.7 nM, respectively. They were more potent than the parent **10a**. The results indicated that substitution at the *para* position of the phenyl ring could increase the potency.

Given the profile of PARP-1 inhibition, compounds **8b**, **8e**, **9e**, **9s**, **10e** and **10f** were selected to evaluate in vitro for their growth inhibitory activity as single agent against human colon cancer cell line HCT116 by SRB assay. Veliparib was used as the positive control and the results were summarized in Table 2. The results indicated that compound **9s** showed almost similar activity to the positive control. Notably, the inhibitory activity of **10e** (27 μM) and **10f** (7.4 μM) were 2.3 and 8.6 fold more potent than veliparib (64 μM), respectively (Table 2). In order to further evaluate these inhibitors as potential agents for chemotherapeutic drugs, these compounds were selected to assess the ability to enhance the cytotoxic effect of chemotherapy agent temozolomide (TMZ) in vitro cellular growth inhibition assays and the calculation of potentiation factors (PF<sub>50</sub>) in A549 cell line. A standard concentration of 0.5 μM PARP-1 inhibitor, which is not intrinsically growth inhibitory, was used. The results were summarized in Table 3. A value

Table 2

The IC<sub>50</sub> value of the selected compounds in HCT116 cells

Compd	IC <sub>50</sub> <sup>a</sup> (HCT116, μM)
<b>8b</b>	>100
<b>8e</b>	>100
<b>9e</b>	>100
<b>9s</b>	65.5
<b>10e</b>	27
<b>10f</b>	7.4
Veliparib	64

<sup>a</sup> The IC<sub>50</sub> value is the concentration required to reduce cell proliferation by 50% in single agent cytotoxicity assay.

Table 3

The potentiation effect of the selected compounds on temozolomide activity in A549 human tumor cell line

Compd	IC <sub>50</sub> <sup>a</sup> (A549, μM)	PF <sub>50</sub> <sup>b</sup>
TMZ	295.0	—
TMZ + veliparib	133.5	2.2
TMZ + <b>8b</b>	338.0	0.9
TMZ + <b>8e</b>	354.0	0.8
TMZ + <b>9e</b>	310.0	1.0
TMZ + <b>9s</b>	151.5	1.9
TMZ + <b>10e</b>	130.5	2.3
TMZ + <b>10f</b>	188.0	1.6

<sup>a</sup> The IC<sub>50</sub> value is the concentration required to reduce cell proliferation by 50% in single agent cytotoxicity assay.<sup>b</sup> The PF<sub>50</sub> value is the potentiation factor, calculated as the ratio of the EC<sub>50</sub> for temozolomide divided by the IC<sub>50</sub> of temozolomide + PARP-1 inhibitor, the test compounds were used at a fixed concentration of 0.5 μM.

of PF<sub>50</sub> greater than 1.0 indicates that the PARP-1 inhibitors are capable of enhancing the effects of cytotoxic agents. Despite potent inhibition of the PARP-1 enzyme, the selected compounds

exhibited a broad array of potentiating efficacy. Compounds **9s**, **10e** and **10f** were capable of enhancing the effect of TMZ in A549 cell line by the PF<sub>50</sub> values of 1.9, 2.3 and 1.6, respectively.

In summary, a series of novel 5-fluorine-benzimidazole-4-carboxamide derivatives were designed, synthesized and biologically evaluated as potent PARP-1 inhibitors. Representative compounds **10e** and **11f** displayed potent in vitro PARP-1 enzymatic inhibition and potent enhancement of cellular growth inhibition. More importantly, Compound **10f** exhibited a significant IC<sub>50</sub> value of 7.4 nM in cellular assay against HCT116 cell line and a profound synergic efficacy combined with temozolomide with PF<sub>50</sub> values of 1.6 against A549 cell line. Further pharmacokinetic evaluation is ongoing and will be reported in the near future.

## Acknowledgments

This work was supported by the National Natural Science Foundation of China (Grant No. 81502928), Outstanding Scientific and Technological Innovation Team of Jiangsu Province of China in 2015 and Fundamental Research Funds for the Central Universities (No. 2015PY015).

## References and notes

- Hassa, P. O.; Hottiger, M. O. *Front. Biosci. Landmark* **2008**, *13*, 3046.
- De, V. M.; Schreiber, V.; Dantzer, F. *Biochem. Pharmacol.* **2012**, *84*, 137.
- Ye, N.; Chen, C. H.; Chen, T.; Song, Z.; He, J. X.; Huan, X. J.; Song, S. S.; Liu, Q.; Chen, Y.; Ding, J.; Xu, Y.; Miao, Z. H.; Zhang, A. J. *Med. Chem.* **2013**, *56*, 2885.
- Xie, Z.; Zhou, Y.; Zhao, W.; Jiao, H.; Chen, Y.; Yang, Y.; Li, Z. *Bioorg. Med. Chem. Lett.* **2015**, *25*, 4557.
- Zhu, Q.; Wang, X.; Chu, Z.; He, G.; Dong, G.; Xu, Y. *Bioorg. Med. Chem. Lett.* **2013**, *23*, 1993.
- Rigakos, G.; Razis, E. *Oncologist* **2012**, *17*, 956.
- Muggia, F.; Safra, T. *Anticancer Res.* **2014**, *34*, 551.
- Tinker, A. V.; Gelmon, K. *Curr. Pharm. Des.* **2012**, *18*, 3770.
- Hannah, F.; Nuala, M.; Christopher, J. L.; Andrew, N. J. T.; Damian, A. J.; Tobias, B. R.; Manuela, S.; Krystyna, J. D.; Ian, H.; Charlotte, K.; Niall, M. B. M.; Stephen, P. J.; Graeme, C. M. S.; Alan, A. *Nature* **2005**, *434*, 917.
- Zhu, Q.; Wang, X.; Hu, Y.; He, X.; Gong, G.; Xu, Y. *Bioorg. Med. Chem.* **2015**, *23*, 6551.
- Coleman, R. L.; Sill, M. W.; Bell-McGuinn, K.; Aghajanian, C.; Gray, H. J.; Tewari, K. S.; Rubin, S. C.; Rutherford, T. J.; Chan, J. K.; Chen, A.; Swisher, E. M. *Gynecol. Oncol.* **2015**, *137*, 386.
- Li, X.; Delzer, J.; Voorman, R.; de Morais, S. M.; Lao, Y. *Drug Metab. Dispos.* **2011**, *39*, 1161.
- Purser, S.; Moore, P. R.; Swallow, S.; Gouverneur, V. *Chem. Soc. Rev.* **2008**, *37*, 320.
- Swallow, S. *Prog. Med. Chem.* **2015**, *54*, 65.
- Gillis, E. P.; Eastman, K. J.; Hill, M. D.; Donnelly, D. J.; Meanwell, N. A. *J. Med. Chem.* **2015**, *58*, 8315.
- General procedure for the synthesis of the target compounds 8a–8e:** (i) A solution of 2,6-difluorobenzoic acid (0.32 mol) in thionyl chloride (100 mL) was heated to reflux for 2 h. The resulting solution was concentrated and acid chloride intermediate was used in the next step without additional purification. To a solution of the acid chloride in anhydrous THF (100 mL) was added ammonium hydroxide (79 mL) at 0 °C. After stirring at room temperature for 0.5 h, the reaction mixture was concentrated under reduced pressure. Then the reaction mixture was poured into cooled water (50 mL), extracted with ethyl acetate (100 mL × 3), and washed with brine (150 mL × 2). The organic layer was dried and concentrated to give the intermediate **2** in 90% yield which used in next step without purification. (ii) To a solution of 2,6-difluorobenzamide (0.28 mol) in concentrated sulfuric acid (90 mL) was added fuming nitric acid (12 mL) by dropwise under 0 °C. The mixture was stirred for 2 h at room temperature. The pH was adjusted to 6 with 30% sodium hydroxide solution, then filtered and the filtrate was extracted with ethyl acetate (100 mL × 3), and washed with brine (150 mL × 2). The organic layer was dried and concentrated in vacuo to give the intermediate **3** as yellow solid in 91.40% yield. (iii) To a solution of 2,6-difluoro-3-nitrobenzamide (0.25 mol) in ethanol (300 mL) was added ammonium hydroxide (25 mL). The reaction mixture was stirred at room temperature overnight and the precipitate was collected by filtration, washed with isopropanol and dried in vacuum to give **4** 31.5 g as yellow solid, yield 77.6%. (iv) A suspension of 2-amino-6-fluoro-3-nitrobenzamide (0.05 mol) in ethanol (100 mL) was reduced by hydrogen in the presence of palladium on carbon (10%, 1.00 g). After stirring at room temperature for 12 h, the reaction mixture was filtered. Solvent was removed under reduced pressure and the residue was subjected to silica gel column chromatography using dichloromethane/methanol (3:1) as eluent to give **5** 5.00 g as light yellow solid, yield 58.9%. (v) To a solution of 3-pipecolic acid (0.06 mol) and 2,3-diamino-6-fluorobenzamide (0.06 mol) in DMF (100 mL) was treated with PyBOP (0.06 mol) and *N,N*-diisopropylethylamine (0.18 mol). The reaction mixture was stirred at room temperature overnight. The solvent was removed using high vacuum. The residue was subjected to flash column chromatography using methylene chloride/methanol (30:1) to give the intermediate **6** as a white solid. The intermediate **6** was dissolved in glacial acetic acid (30 mL) and refluxed for 4 h until the reaction was complete (monitoring by TLC). The solvent was removed and the solid residue was purified by column chromatography using methylene chloride/methanol (80:1) as eluent to give pure **7a–7e** in 50–72% yield. (vi) A solution of **7a–7e** (25 mmol) in methanol (100 mL) was reduced with hydrogen in the presence of palladium on carbon (10%, 1.00 g). After stirring at room temperature for 12 h, the reaction mixture was filtered, and the filtrate was concentrated to give pure target compounds **8a–8e** in 52–80% yield.
- General procedure for the synthesis of the target compounds 9a–9y:** (i) A solution of **8a–8e** (2 mmol) in MeOH (10 mL) was stirred with formaldehyde, acetone or propionaldehyde at room temperature overnight. Sodium cyanoborohydride was added and the solution stirred at room temperature for 3 h. After concentration, the residue was purified by column chromatography using methylene chloride/methanol (80:1 to 20:1) as eluent to give the target compounds **9a–9t** in 60–94% yield. (ii) To a solution of **8a–8e** (2 mmol) in dichloromethane (10 mL) was added trimethylamine and acetylchloride at 0 °C. The mixture was stirred at room temperature for 2 h and purified by column chromatography using methylene chloride/methanol (80:1 to 20:1) as eluent to give the target compounds **9u–9y** in 82–90% yield.
- General procedure for the synthesis of the target compounds 10a–10f:** (i) To a solution of 2,3-diamino-6-fluorobenzamide (8.80 mmol) in methanol was added the intermediate aromatic aldehyde (8.80 mmol) and NaHSO<sub>3</sub> (8.80 mmol). The mixture was stirred at reflux temperature for 12 h, the solid was collected by filtration and washed with methanol to give the target compounds **10a–10e** in 40–67% yield. (ii) To a solution of **5** (8.87 mmol) in methanol (20 mL) was added the intermediate 4-(*N*-Boc-piperidine) benzaldehyde (8.87 mmol) and NaHSO<sub>3</sub> (8.87 mmol). The mixture was stirred at reflux temperature for 12 h, the solid was collected by filtration and washed with methanol to give intermediate **11** in 64% yield. A solution of **11** (5.69 mmol) in a mixture of THF (10 mL) and methanol (10 mL) was treated with concentrated HCl (5 mL) and stirred at room temperature for 2 h. The resulting precipitate was collected by filtration and dried to give target compound **10f** in 62.5% yield.
- Analytical data for selected final compound 8b:** Mp: 226–228 °C. <sup>1</sup>H-NMR (300 MHz, DMSO-*d*<sub>6</sub>) δ (ppm): 1.52 (s, 3H, –CH<sub>3</sub>), 1.60–1.62 (m, 1H, –CH–), 1.73–1.81 (m, 2H, –CH<sub>2</sub>–), 2.33–2.39 (m, 1H, –CH–), 2.79–2.83 (m, 1H, NCH–), 3.02–3.08 (m, 1H, –NCH–), 7.05 (dd, *J* = 12.09, 8.81 Hz, 1H, ArH), 7.60 (q, *J* = 4.35 Hz, 1H, ArH), 7.70 (s, 1H, –CONH<sub>2</sub>). <sup>13</sup>C NMR (75 MHz, DMSO-*d*<sub>6</sub>) δ (ppm): 22.08, 22.97, 36.43, 43.83, 64.97, 111.94, 118.14, 134.00, 136.64, 154.96, 155.09, 158.21, 163.78. HRMS-ESI *m/z* [M+H]<sup>+</sup>: calcd for C<sub>13</sub>H<sub>16</sub>FN<sub>4</sub>O: 263.1308, found: 263.1304.
- Analytical data for selected final compound 10f:** Mp: 232–234 °C. <sup>1</sup>H NMR (300 MHz, DMSO-*d*<sub>6</sub>) δ (ppm): 3.22 (s, 4H, –(CH<sub>2</sub>)<sub>2</sub>–), 3.67 (s, 4H, –(CH<sub>2</sub>)<sub>2</sub>–), 7.23 (d, *J* = 9.06 Hz, 2H, ArH), 7.38 (t, *J* = 10.74 Hz, 1H, ArH), 7.81 (q, *J* = 4.32 Hz, 1H, ArH), 8.04 (s, 1H, piperazine-H), 8.28 (d, *J* = 8.88 Hz, 2H, ArH), 8.35 (s, 1H, imidazole-H), 9.51 (s, 2H, CONH<sub>2</sub>). <sup>13</sup>C NMR (75 MHz, DMSO-*d*<sub>6</sub>) δ (ppm): 42.16, 43.56, 110.86, 111.17, 111.53, 113.82, 114.36, 115.98, 116.11, 128.93, 130.35, 151.24, 152.91, 154.66, 157.91, 162.55. HRMS-ESI *m/z* [M+H]<sup>+</sup>: calcd for C<sub>18</sub>H<sub>19</sub>FN<sub>5</sub>O: 340.1574, found: 340.1541.